

Level inversion in kaonic nuclei and the high-density nuclear equation of state

Rong-Yao Yang, Wei-Zhou Jiang, Si-Na Wei

School of Physics, Southeast University, Nanjing 211189, China

Abstract

It is very difficult for any nuclear model to pin down the saturation property and high-density equation of state (EOS) simultaneously because of high nonlinearity of the nuclear many-body problem. In this work, we propose, for the first time, to use the special property of light kaonic nuclei to characterize the relation between saturation property and high-density EOS. With a series of relativistic mean-field models, this special property is found to be the level inversion between orbitals $2S_{1/2}$ and $1D_{5/2}$ in light kaonic nuclei. This level inversion can serve as a theoretical laboratory to group the incompressibility at saturation density and the EOS at supra-normal densities simultaneously.

Keywords: kaonic nuclei, equation of state, relativistic mean-field theory

PACS: 21.65.Mn, 13.75.Jz, 21.10.Gv, 21.60.Gx

1. Introduction

The determination of the nuclear equation of state (EOS) with certain accuracy is crucial for the understanding of the phenomena related to relativistic heavy-ion collisions [1] and astrophysical objects, such as, neutron stars [2, 3], gravity waves [4], etc. Due to the high nonlinearity of the nuclear many-body problems, some critical uncertainties still exist in the nuclear EOS after decades of effort. For instance, the large uncertainty of the high-density EOS in symmetric nuclear matter still has a large relative error of 50% as extracted from the data of the heavy-ion collisions [5]. This large error not only prevents one from extracting accurate structural information, such as the phase structures and transitions, but also makes it more difficult to pin down the huge divergency in symmetry energy at high densities [1]. Though the high nuclear density can naturally form in central neutron stars, neither can the celestial data give a sufficiently satisfactory constraint on the high-density EOS [1, 6].

Another important quantity of the nuclear EOS is the incompressibility at saturation density [7, 8]. In the past, significant progress has been achieved in constraining the incompressibility by analyzing the experimental data, such as the nuclear masses, nuclear radii and giant monopole resonance [9, 10, 11, 12, 13, 14, 7, 15, 8], etc. The most proposed value for the incompressibility is around 230 MeV, such as 230 ± 40 MeV given in Ref. [14], while higher values in the range of 250-315 MeV can not be ruled out after a comprehensive reanalysis of the data on giant monopole resonances [7]. Note that our work does not aim at narrowing down or excluding some range of the incompressibility. Actually, this large uncertainty provides us a parameter space to do the readjustment in the study of the EOS.

Confronting the large uncertainty of the high-density EOS, one would like to know whether there exist the sensitive probes, based on the nuclear structure properties, to reduce it. On the other hand, the high-density EOS should be connected to the EOS near or beneath the saturation density, though

arXiv:1906.10868v1 [nucl-th] 26 Jun 2019

the predictive power of nuclear models is weak in the whole density region for the high nonlinearity of the in-medium strong interaction. One may ask naturally: What is the relationship between the incompressibility at saturation density and the EOS at high densities? It is also very interesting to reveal what role of such a relationship can be played in constraining the EOS at saturation and high densities mutually. The key point to study these problems is firstly to have a finite candidate with a high-density core that concerns the high-density EOS.

In fact, the kaonic nuclei are a good candidate that can feature a dense core at supra-normal density [16, 17]. It is theoretically feasible to employ structural properties of kaonic nuclei that encompass the information of a large density range to impose a global constraint on the EOS both in the lower-density and higher-density regions. Compared with the data at high densities extracted from heavy-ion collisions, the structural properties in the ground state of kaonic nuclei should be more precise for probing the high-density EOS. In the past, we have actually made some efforts to establish the correlation between the low-density halo phenomenon in kaonic nuclei and the stiffness of EOS at saturation and high densities [18]. In this work, we further investigate the ground-state properties of kaonic nuclei in the framework of relativistic mean-field (RMF) theory. It is one of our aims to explore the relationship between the incompressibility and the stiffness of the high-density EOS by singling out some special structural information in kaonic nuclei. We will find that the level inversion characteristic in light kaonic nuclei is tightly related to incompressibility, the stiffness of the high-density EOS, and the relationship between. In the following, we in turn give the formalism, results and discussions, and the summary in sect. II-IV.

2. Formalism

In kaonic nuclei, the binding of the antikaon is given by its additive couplings with scalar and vector mesons, whereas this is apart from the nucleonic binding in normal nuclei that is a cancellation of the scalar and vector potentials. Such a deep binding in kaonic nuclei results in correspondingly much deeper nucleonic potential due to the coupling between the antikaon and nucleons, giving rise to exotic features such as the dense core at supra-normal density [16, 17] and diffusive halo [18]. Here, we adopt the RMF theory to investigate the ground-state properties of kaonic nuclei and its relationship with the nuclear EOS. The Lagrangian density for nucleons is generally given by

$$\begin{aligned} \mathcal{L}_0 = & \bar{\psi}_B [i\gamma_\mu \partial^\mu - M_B + g_\sigma \sigma - g_\omega \gamma_\mu \omega^\mu - g_\rho \gamma_\mu \tau_3 b_0^\mu - e \frac{1 + \tau_3}{2} \gamma_\mu A^\mu] \psi_B - \frac{1}{4} F_{\mu\nu} F^{\mu\nu} + \frac{1}{2} m_\omega^2 \omega_\mu \omega^\mu \\ & - \frac{1}{4} B_{\mu\nu} B^{\mu\nu} + \frac{1}{2} m_\rho^2 b_{0\mu} b_0^\mu - \frac{1}{4} A_{\mu\nu} A^{\mu\nu} + \frac{1}{2} (\partial_\mu \sigma \partial^\mu \sigma - m_\sigma^2 \sigma^2) + U(\sigma, \omega^\mu), \end{aligned} \quad (1)$$

where ψ_B , σ , ω_μ , $b_{0\mu}$, A_μ represent the baryon, scalar, vector, isovector vector, electromagnetic field, respectively. The g_i ($i = \sigma, \omega, \rho$) is the corresponding coupling constants between meson fields and nucleons. The M_B , m_σ , m_ω , m_ρ are the masses for baryon and corresponding mesons. The $\tau_3 = \pm 1$ for protons and neutrons, respectively. The strength tensors of the ω , ρ meson and the photon are defined as $F_{\mu\nu} = \partial_\mu \omega_\nu - \partial_\nu \omega_\mu$, $B_{\mu\nu} = \partial_\mu b_{0\nu} - \partial_\nu b_{0\mu}$, $A_{\mu\nu} = \partial_\mu A_\nu - \partial_\nu A_\mu$.

The self-interacting terms are expressed as

$$U(\sigma, \omega^\mu) = -\frac{1}{3} g_2 \sigma^3 - \frac{1}{4} g_3 \sigma^4 + \frac{1}{4} c_3 (\omega_\mu \omega^\mu)^2, \quad (2)$$

with g_2 , g_3 denoting the strength of the nonlinear terms of scalar field. The c_3 is the parameter for the non-linear ω self-coupling term with which the stiffness of the nuclear EOS at high densities can be readjusted sensitively. In the RMF approximation [19], it is easy to deduce the EOS for nuclear

matter and the equation of motion for nucleons in a nucleus. The sound velocity square v_s^2 is defined as $v_s^2 = \partial P / \partial \epsilon$ being the partial derivative of the pressure with respect to the energy density, and it can be used to measure the stiffness of the nuclear EOS.

To investigate kaonic nuclei, we should incorporate the Lagrangian density describing the strong attraction between the nucleons and K^- mesons. The Lagrangian density for kaons is written as [20]

$$\mathcal{L}_{KN} = (\mathcal{D}_\mu K)^\dagger (\mathcal{D}^\mu K) - (m_K^2 - g_{\sigma K} m_K \sigma) K^\dagger K, \quad (3)$$

where the covariant derivative is defined as $\mathcal{D}_\mu \equiv \partial_\mu + iV_\mu$ with $V_\mu = g_{\omega K} \omega_\mu + g_{\rho K} b_{0\mu} + e \frac{1+\tau_3}{2} A_\mu$. Here, $K = K^+$ and $K^\dagger = K^-$ instead of kaonic doublets since in kaonic nuclei it is just a K^- meson implanted into a nucleus without neutral kaons. It can be inferred from Eq.(3) that the strongly attractive K^-N interaction is mediated by σ , ω , ρ meson fields and electromagnetic field. This strong attraction is responsible for the deep binding of the kaonic nuclei.

Combining the Lagrangian density for nucleons in Eq. (1) and K^- mesons in Eq. (3), we can write out the RMF equations of motion as follows

$$[-i\boldsymbol{\alpha} \cdot \boldsymbol{\nabla} + \beta(M_B - g_\sigma \sigma) + g_\omega \omega + g_\rho \tau_3 b_0 + e \frac{1+\tau_3}{2} A] \psi_B = E \psi_B, \quad (4)$$

$$(-\nabla^2 + m_K^2 - E_{K^-}^2 + \Pi) K^- = 0, \quad (5)$$

$$(-\nabla^2 + m_\phi^2) \phi = s_\phi, \quad (6)$$

where the s_ϕ denotes the source term for mesons or photon ($m_A = 0$)

$$s_\phi = \begin{cases} g_\sigma \rho_s - g_2 \sigma^2 - g_3 \sigma^3 + g_{\sigma K} m_K K^- K^+, & \phi = \sigma, \\ g_\omega \rho_v - c_3 \omega^3 - g_{\omega K} \rho_{K^-}, & \phi = \omega, \\ g_\rho \rho_3 - g_{\rho K} \rho_{K^-}, & \phi = b_0, \\ e \rho_p - e \rho_{K^-}, & \phi = A. \end{cases} \quad (7)$$

Here ρ_s , ρ_v , ρ_3 , ρ_p are the scalar, vector, isovector, and proton density, respectively. ρ_{K^-} is the K^- density [21]

$$\rho_{K^-} = 2(E_{K^-} + g_{\omega K} \omega + g_{\rho K} b_0 + eA) K^- K^+. \quad (8)$$

E and E_{K^-} are the energy eigenvalues for nucleons and K^- meson, respectively. The K^- self-energy term is expressed as

$$\Pi = -g_{\sigma K} m_K \sigma - 2E_{K^-} V - V^2, \quad (9)$$

where $V = g_{\omega K} \omega + g_{\rho K} b_0 + \frac{1+\tau_3}{2} eA$. The parameters for K^- are adapted to the K^- optical potential which is defined as $U_{opt}(\mathbf{p}, \rho_0) = \omega(\mathbf{p}, \rho_0) - \sqrt{\mathbf{p}^2 + m_K^2}$ with $\omega(\mathbf{p}, \rho_0)$ being the in-medium energy at saturation density [22].

Solving these equations of motion with an iterative method, one can calculate the ground-state properties of normal nuclei and kaonic nuclei after the parametrizations are chosen. More detailed information can be referred to Ref. [21].

3. Results and discussions

Prior to giving the numerical results, we first elaborate the parametrization. For the nucleonic sector, we take some best-fit non-linear RMF models that fit the saturation properties of symmetric nuclear matter and the ground-state properties of typical spherical nuclei. For the kaonic sector, the determination of the parameters $g_{\omega K}$ and $g_{\rho K}$ in Eq. (3) can resort to the SU(3) relation:

$2g_{\omega K} = 2g_{\rho K} = g_{\rho\pi} = 6.04$, and the $g_{\sigma K}$ is adjusted to the K^- optical potential. Up to now, there is no consensus on the depth of K^- optical potential. Experimentally, it can be extracted from the data of kaonic atoms [23, 24, 25, 26, 27, 28], K^-N scatterings [33, 34, 29, 30, 31, 32] and heavy-ion collisions [22, 35, 36, 37, 38, 39]. Because the data from the K^-N scatterings and kaonic atoms mainly reflect the low-density feature of K^-N interaction, one needs some specific extrapolations to get the depth at saturation density. Unfortunately, the extrapolated values are largely model dependent, ranging from -200 MeV to -50 MeV [23, 24, 25, 26, 27, 28, 33, 34, 29, 30, 31, 32]. On the other hand, the heavy-ion collisions can produce an almost consistent K^- potential depth around -100 MeV at saturation density [22, 35, 36, 37, 38, 39]. Hence, we adopt -100 MeV as the K^- optical potential depth at saturation density [22] to fit the kaonic parameters. We should mention that the effects from the K^- absorption by nucleons can be included by introducing an imaginary potential into the K^- self-energy term Π in Eq. (9) [40, 41, 20]. It is found that the inclusion of the imaginary potential has little effect on the final results in our parametrizations and does not ever affect the conclusion of this work. Therefore, we will not deal with the imaginary part in detail hereafter.

Firstly, we adopt NL3 parameter [42] for nucleons in Eq. (1) to explore the ground-state properties in kaonic nuclei. Displayed in Fig. 1 are the nucleon potentials and nuclear densities in ^{18}O and $^{18}_{K^-}O$. Due to the strong attraction between nucleons and K^- mesons, the nucleon potential in kaonic nuclei is greatly changed by the implantation of the K^- meson. We can see that the nucleon potential in kaonic nucleus $^{18}_{K^-}O$ is much deeper than that in normal nucleus ^{18}O in the core region ($r < 2fm$). Its direct consequence is that the nuclear density in the core of $^{18}_{K^-}O$ is over two times the saturation density, dramatically larger than that of ^{18}O . We notice that the implanted K^- meson is almost squeezed in the core region where the huge variation in the nucleon potential takes place consistently, as seen in Fig. 1. For comparison, we present in Fig. 1 the results for two orbital occupation orders in $^{18}_{K^-}O$: one with the out-most two neutrons occupying the orbital $1D_{5/2}$ and the other occupying orbital $2S_{1/2}$. As can be seen, the latter corresponds to a higher nuclear density and a deeper nucleon potential in the core region which may imply that the occupation order with the out-most orbital $2S_{1/2}$ is energetically favorable. It is checked explicitly that the total binding energy of $^{18}_{K^-}O$ with the out-most orbital being $2S_{1/2}$ is truly larger than that with the out-most orbital being $1D_{5/2}$. In this case, the ground state of $^{18}_{K^-}O$ is affirmed to have the occupation order whose out-most orbital is the $2S_{1/2}$. Together with the internal level shifts, the level ordering appears to be different from Mayer's shell model.

In Fig. 2, we show the energy levels for neutrons in Oxygen isotopes, ^{40}Ca and their corresponding kaonic nuclei. Indeed, the orders of energy levels in all these kaonic nuclei are not the same as Mayer's shell model: the orbital $2S_{1/2}$ obviously bounds deeper than the orbital $1D_{5/2}$. It appears that orbitals $1P_{1/2}$, $2S_{1/2}$ and $1D_{5/2}$ form a new shell in kaonic nuclei. In these cases, the magic number is simultaneously changed. We also calculated the ground-state properties for $^{32}_{K^-}S$, $^{42}_{K^-}Ca$, $^{44}_{K^-}Ca$, etc., and found that the downward shift of $S_{1/2}$ orbitals is very general in kaonic nuclei. As this level-inversion phenomenon does exist pervasively in light and intermediate-light kaonic nuclei, it is necessary to reveal the underlying mechanism responsible for the very phenomenon and the corresponding spectra specific for kaonic nuclei.

The phenomenon of the downward shift of $S_{1/2}$ orbitals can be understood from the corresponding schrödinger-like equation for the big component of nucleon's Dirac equation Eq. (4). To solve the Dirac equation, we introduce the quantum number set for a spherical nucleus which is $\{n, \kappa, m, t\}$ where n is the principle quantum number, m is the magnetic quantum number, and t denotes the isospin. κ is the eigenvalue of a conserved operator \mathbf{K} with $\mathbf{K} \equiv -\gamma^0(\boldsymbol{\Sigma} \cdot \mathbf{L} + 1)$, measuring the spin-orbit coupling. With these quantum numbers, the four-component Dirac spinor can be divided

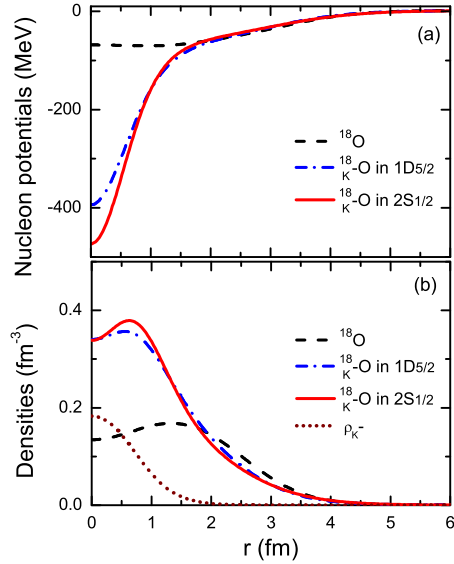


Figure 1: (Color online) The nucleon potentials and nuclear densities in ^{18}O (dashed curves) and $^{18}_{K^-}\text{O}$ (dash-dotted and solid curves). The labels "1D $_{5/2}$ " and "2S $_{1/2}$ " denote the out-most two neutrons occupying orbitals 1D $_{5/2}$ and 2S $_{1/2}$, respectively. In the lower panel, the K^- density distribution ρ_{K^-} is obtained with the out-most neutrons occupying orbital 2S $_{1/2}$.

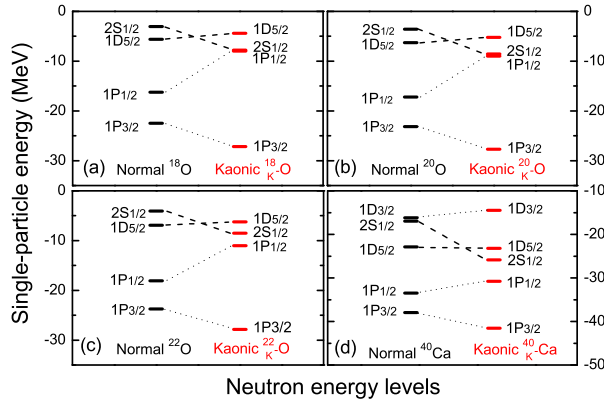


Figure 2: (Color online) The energy levels for neutrons in Oxygen isotopes, ^{40}Ca and their corresponding kaonic nuclei.

into two components,

$$\psi_{n\kappa mt}(r) = \left\{ \begin{array}{l} i \frac{G_a(r)}{r} \Phi_{\kappa, m} \\ -\frac{F_a(r)}{r} \Phi_{-\kappa, m} \end{array} \right\} \chi_t, \quad (10)$$

where $G_a(r)$ and $F_a(r)$ are the big and small components of the (radial) spinor, respectively. $\{a\} = \{n, \kappa, t\}$, Φ is the spinor spherical harmonic, and χ_t is the isospinor with $t = \pm 1$ for protons and neutrons, respectively. Substituting Eq. (10) into the Dirac equation Eq. (4), the corresponding Schrödinger-like equations for the big component can be obtained as

$$\left[\frac{d^2}{dr^2} - \frac{\kappa(\kappa + 1)}{r^2} + \frac{1}{U_G} \frac{d\Delta}{dr} \frac{d}{dr} + \frac{1}{U_G} \frac{d\Delta}{dr} \frac{\kappa}{r} - U_G U_F \right] G_a(r) = 0, \quad (11)$$

where $U_G = M_B + E - \Delta$, $U_F = M_B - E + \Sigma$, and $\Sigma = V(r) + S(r)$, $\Delta = V(r) - S(r)$ with $V(r) = g_\omega \omega + g_\rho \tau_3 b_0 + eA(1 + \tau_3)/2$, and $S(r) = -g_\sigma \sigma$. As the $\kappa = -1$ for S $_{1/2}$ orbitals, the repulsive

centrifugal barrier (CB) vanishes as $\kappa(\kappa + 1)/r^2=0$. Then, there is no repulsive force contributed from CB to counteract the strongly attractive interaction induced by K^- meson in the core region of kaonic nuclei. Naturally, the $S_{1/2}$ orbitals are driven greatly downward by the implanted K^- meson. The level inversion may occur for enough downwards shift of the $S_{1/2}$ orbital. For instance, the level inversion between orbitals $2S_{1/2}$ and $1D_{5/2}$ is very prominent in light kaonic nuclei. We notice that the downward shift of $S_{1/2}$ orbitals becomes shallower for heavier kaonic nuclei since the K^- meson will be pulled outwards by the strong attraction provided by more and more out-layer nucleons. Consistently, a shallower nucleon potential appears near the center of heavier kaonic nuclei. Consequently, the $2S_{1/2} - 1D_{5/2}$ inversion diminishes in intermediate-mass kaonic nuclei and will vanish in heavy kaonic nuclei.

From Fig. 2, we can also observe that the spin-orbit splitting of orbitals $1P_{3/2}$ and $1P_{1/2}$ in kaonic nuclei is obviously larger than that in corresponding normal nuclei. This is attributed to the enhanced spin-orbit potential due to the implantation of the K^- meson, while the latter provides an additional strong attraction to deepen the nucleon potential and hence increase the radial gradient of the potential that accounts for the spin-orbit potential. Consequently, it makes the spin-orbit splitting of the $1P_{3/2}$ and $1P_{1/2}$ orbitals in kaonic nuclei much larger than that of normal nuclei. Here, we stress that the downward shift of $S_{1/2}$ orbitals dominates the level re-orderings including the level inversion and the change of the spin-orbit splittings. The similar role of $2S_{1/2}$ orbital in influencing the energy levels was pointed out in Refs [43, 44]. Especially, it was found that the occupation of $2S_{1/2}$ proton orbital plays an important role in enhancing the $P_{3/2} - P_{1/2}$ splitting of neutron orbitals in ^{48}Ca as compared to ^{46}Ar [43]. We should, however, note that the underlying mechanism and the consequence for the shift of $S_{1/2}$ orbitals are quite different in this work. The large shift here does change the normal order of energy levels, while it does not in the normal nuclei. More importantly, the occupation of $S_{1/2}$ orbitals in normal nuclei has nothing to do with the high-density core that is only subject to the additional strong attraction provided by the K^- implantation. The large shift of $S_{1/2}$ orbitals pulled down by K^- meson actually reflects a result of the compression that may give rise to a core density up to twice the saturation density. The kaonic nuclei can thus be a possible platform to reveal the effects of different high-density EOS's by virtue of theoretical signals such as the downward shift of $S_{1/2}$ orbitals, the broadened spin-orbit splitting of $1P$ orbitals, and other structural changes in kaonic nuclei.

The effects of high-density EOS can be reflected in the structural characteristic of kaonic nuclei since the aforementioned downward shift of $S_{1/2}$ orbitals could produce supra-normal nuclear density near the center. Additionally, the incompressibility should also be an important factor which would have considerable impact on the nucleon potential. It is thus very meaningful to study the relationships between the ground-state properties of kaonic nuclei and the incompressibility and high-density stiffness of the nuclear EOS. In the following, we will firstly obtain a series of EOS's with different incompressibility and stiffness at high densities. Then, the corresponding parameters are used to calculate the ground-state properties of kaonic nuclei. To simulate different EOS's systematically, we set the masses in Eq.(1) the same as that of NL3 [42]. With a given c_3 , the coupling constants including g_σ , g_ω , g_2 , g_3 are fitted to the saturation properties, including the energy per baryon -16.3 MeV at saturation density $\rho_0 = 0.148\text{fm}^{-3}$, the effective mass of nucleon M_B^*/M_B around 0.6 and a given incompressibility (adjustable). Generally, a larger c_3 would produce a softer EOS. These simple treatments could produce a series of EOS's with the different incompressibility or different stiffness (sound velocity square) at high densities. Though these parameter sets are not obtained by the best-fit procedure, the good accuracy in simulating the properties of finite nuclei is comparable to those best-fit parameter sets. At the same time, the main conclusion in this paper is not affected by the strategy of choosing the base EOS. Based on these obtained nuclear EOS's, we can calculate

the ground-state properties of kaonic nuclei and its relationship with the nuclear EOS. By doing so, a clear connection can be built between the nuclear EOS and the phenomenon of level inversion in kaonic nuclei.

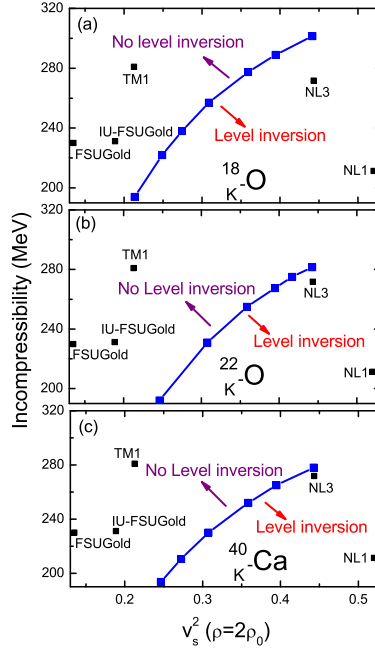


Figure 3: (Color online) The phase diagram for the level inversion in $^{18}_{K^-}O$, $^{22}_{K^-}O$ and $^{40}_{K^-}Ca$ in the incompressibility-stiffness plane. Here, we use the sound velocity square (the partial derivative of the pressure with respect to the energy density) at $2\rho_0$ as a criterion of the EOS's stiffness at high density.

Using $^{18}_{K^-}O$, $^{22}_{K^-}O$ and $^{40}_{K^-}Ca$ as examples, we show in Fig. 3 the critical level inversion in the incompressibility-stiffness plane. It is found that there exists critical boundary to separate the system with and without the level inversion. As can be seen from Fig. 3, the level inversion will occur for a stiff EOS at high densities combined with a relative small incompressibility (on the lower right side of the critical boundary in each panel), while it does not occur for a relative soft EOS at high densities combined with a large incompressibility (on the upper left side of the boundary). This result is understandable since the level inversion is dominated by the downward shift of $S_{1/2}$ orbitals which is tightly related to considerable compression near the center of kaonic nuclei induced by the strong K^-N attraction. A smaller incompressibility means easier compression, and a stiffer EOS corresponds to a deeper K^-N attraction at high densities as the interactions mediated by scalar and vector mesons are coherently attractive. For the EOS's above critical boundary, the downward shift of $S_{1/2}$ orbitals remains, but the $2S_{1/2}$ orbital becomes less bound than the $1D_{5/2}$ orbital.

According to the incompressibility and the $2\rho_0$ sound velocity square of the model, we mark in Fig. 3 the positions for several best-fit parameter sets, such as FSUGold [45], IU-FSUGold [46], NL1 [47], TM1 [48], etc. The allocation of these parameter sets on the both sides of the critical boundary is consistent with their predication on the situation of the $2S_{1/2} - 1D_{5/2}$ inversion in $^{18}_{K^-}O$, $^{22}_{K^-}O$ and $^{40}_{K^-}Ca$. Namely, the level-inversion phenomenon appears with the parameter sets NL1 and NL3, while it does not appear with the FSUGold, IU-FSUGold, and TM1. Hence, nuclear EOS's can be divided into different groups by this critical boundary in the incompressibility-stiffness plane. As seen in Fig. 3, the critical boundaries obtained from different kaonic nuclei are similar with each

other, whereas the differences between each curve are subject to the difference of nucleon potentials in ^{18}O , ^{22}O and ^{40}Ca . The critical boundary can be shifted moderately when the parameter sets are refitted to a different nucleon effective mass that may affect the density of the energy level. The shift may also be caused by the corresponding modification of the nucleon potential. Nevertheless, these critical boundaries can give the same grouping for different EOS's. Here, we can see that the level inversion needs a stiffer EOS at high densities combined necessarily with a relatively smaller incompressibility, while a softer EOS at high densities with larger incompressibility declines the occurrence of the level inversion. If the level inversion does not occur, the natural combination should be a stiffer EOS at high densities with larger incompressibility or a softer EOS with smaller incompressibility.

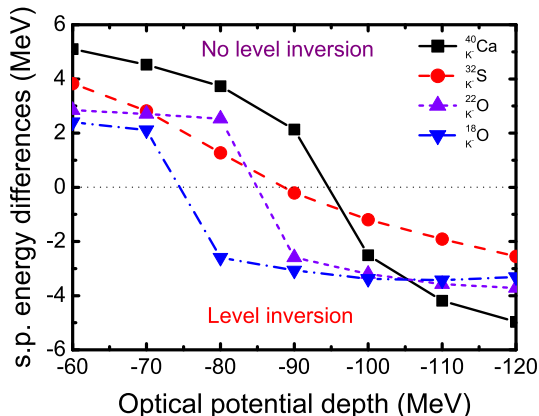


Figure 4: (Color online) The single-particle energy differences between $2S_{1/2}$ and $1D_{5/2}$ orbitals as a function of the depth of K^- optical potential at saturation for $^{40}_{K^-}\text{Ca}$, $^{32}_{K^-}\text{S}$, $^{22}_{K^-}\text{O}$, and $^{18}_{K^-}\text{O}$. Here, the RMF parameter set NL3 is adopted in the calculation.

To investigate the influence of the K^- optical potential depth, we display in Fig. 4 the single-particle (s.p.) energy differences between $2S_{1/2}$ and $1D_{5/2}$ orbitals as a function of the depth of K^- optical potential at saturation for $^{40}_{K^-}\text{Ca}$, $^{32}_{K^-}\text{S}$, $^{22}_{K^-}\text{O}$, and $^{18}_{K^-}\text{O}$. The level inversion requires a deep potential provided by the attraction of K^- . As clearly seen in Fig. 4, there are large parameter spaces especially for light kaonic nuclei allowing the occurrence of the level inversion. In fact, the level inversion will occur inevitably after the K^- optical potential exceeds the threshold. This threshold becomes larger for heavier nuclei, as this is a result of the dilution of the K^- strong attraction by more and more nucleons. For light kaonic nuclei, the threshold can be smaller significantly. For a particular kaonic nucleus, the critical boundary in Fig. 3 will shift moderately to the upper left (lower right) side for deeper (shallower) K^- optical potential. Interestingly, we also find that kaonic nuclei as light as $^{14}_{K^-}\text{C}$ have a similarly large parameter space for the $2S_{1/2} - 1P_{1/2}$ inversion. Accordingly, a large parameter space including the atomic number allows one to choose appropriate kaonic nuclei with the manifest level inversion to group different EOS's, though the depth of the K^- optical potential should be unique and eventually extracted from data.

Knowing that kaonic nuclei are yet to be verified experimentally, we have focused in this work on the special properties of kaonic nuclei and their implication to the EOS especially at high densities. These theoretical results suggest that the experiments to either identify or exclude the kaonic nuclei are very necessary and valuable. We hope the further experiments [49, 50] could bring us affirmative information on this subject in the future.

4. Summary

We have investigated the ground-state properties in kaonic nuclei and its relationship with the nuclear EOS in the framework of RMF theory. Owing to the strong attraction between nucleons and K^- meson, supra-normal nuclear density appears near the center of kaonic nuclei, and the structure of energy levels in kaonic nuclei becomes different from Mayer's shell model. The most striking feature is that the $S_{1/2}$ orbitals shift downwards significantly and the inversion between $2S_{1/2}$ and $1D_{5/2}$ orbital may occur. This level inversion phenomenon is intimately related to the incompressibility and the stiffness of the nuclear EOS at high densities. Specifically, according to the level inversion in kaonic nuclei, there exists a critical boundary in the incompressibility-stiffness plane to divide the nuclear EOS into different groups. The normal level order without the inversion supports a natural combination: the stiffer EOS at high densities with larger incompressibility or the softer EOS with smaller incompressibility, while the occurrence of the level inversion agrees with the combination of stiffer EOS at high densities and smaller incompressibility. These findings provide us theoretical tools to understand/constrain the nuclear EOS in the whole density region.

Acknowledgements

The work was supported in part by the National Natural Science Foundation of China under Grant Nos. 11775049 and 11275048.

References

- [1] B.A. Li, L.W. Chen, C.M.Ko, Phys. Rep. 464 (2008) 113.
- [2] A. Akmal, V.R. Pandharipande, D.G. Ravenhall, Phys. Rev. C 58 (1998) 1804.
- [3] J.M. Lattimer, M. Prakash, Phys. Rep. 442 (2007) 109.
- [4] E. Annala, T. Gorda, A. Kurkela, A. Vuorinen, Phys. Rev. Lett. 120 (2018) 172703.
- [5] P. Danielewicz, R. Lacey, W.G. Lynch, Science 298 (2002) 1592.
- [6] A.W. Steiner, J.M. Lattimer, E.F. Brown, Astrophys. J. 722 (2010) 33.
- [7] J.R. Stone, N.J. Stone, S.A. Moszkowski, Phys. Rev. C 89 (2014) 044316.
- [8] X. Roca-Maza, N. Paar, Prog. Part. Nucl. Phys. 101 (2018) 96.
- [9] J.P. Blaizot, Phys. Rep. 64 (1980) 171.
- [10] D.H. Youngblood, H.L. Clark, Y.W. Lui, Phys. Rev. Lett. 82 (1999) 691.
- [11] B.G. Todd-Rutel, J. Piekarewicz, Phys. Rev. Lett. 95 (2005) 122501.
- [12] P. Klupfel, P.G. Reinhard, T.J. Burvenich, J.A. Maruhn, Phys. Rev. C 79 (2009) 034310.
- [13] A.W. Steiner, J.M. Lattimer, E.F. Brown, Astrophys. J. (2010) 722 33.
- [14] E. Khan, J. Margueron, I. Vidana, Phys. Rev. Lett. 109 (2012) 092501.
- [15] N. Wang, M. Liu, L. Ou, Y.X. Zhang, Phys. Lett. B 751 (2015) 553.

- [16] T. Yamazaki, Y. Akaishi, Phys. Lett. B 353 (2002) 70.
- [17] Y. Akaishi, T. Yamazaki, Phys. Rev. C 65 (2002) 044005.
- [18] R.Y. Yang, W.Z. Jiang, S.N. Wei, Sci. Rep. 7 (2017) 16695.
- [19] B.D. Serot, J.D. Walecka, Adv. Nucl. Phys. 16 (1986) 1.
- [20] D. Gazda, E. Friedman, A. Gal, J. Mareš, Phys. Rev. C 76 (2007) 055204.
- [21] R.Y. Yang, W.Z. Jiang, D.R. Zhang, S.N. Wei, Eur. Phys. J. A 50 (2014) 188.
- [22] Z.Q. Feng, W. J. Xie, G.M. Jin, Phys. Rev. C 90 (2014) 064604.
- [23] C.J. Batty, Nucl. Phys. A 372 (1981) 418.
- [24] E. Friedman, A. Gal, C.J. Batty, Nucl. Phys. A 579 (1994) 518.
- [25] C.J. Batty, E. Friedman, A. Gal, Phys. Rep. 287 (1997) 385.
- [26] E. Friedman, A. Gal, J. Mareš, A. Cieplý, Phys. Rev. C 60 (1999) 024314.
- [27] A. Gal, Nucl. Phys. A 691 (2001) 268C.
- [28] E. Friedman, A. Gal, Phys. Rep. 452 (2007) 89.
- [29] J. Schaffner-Bielich, I.N. Mishustin, J. Bondorf, Nucl. Phys. A 625 (1997) 325.
- [30] A. Ramos, E. Oset, Nucl. Phys. A 671 (2000) 481.
- [31] A. Cieplý, E. Friedman, A. Gal, J. Mareš, Nucl. Phys. A 696 (2001) 173.
- [32] A. Cieplý, E. Friedman, A. Gal, D. Gazda, J. Mareš, Phys. Lett. B 702 (2011) 402.
- [33] T. Waas, N. Kaiser, W. Weise, Phys. Lett. B 365 (1996) 12.
- [34] T. Waas, M. Rho, W. Weise, Nucl. Phys. A 617 (1997) 449.
- [35] G.Q. Li, C.H. Lee, G.E. Brown, Phys. Rev. Lett. 79 (1997) 5214.
- [36] W. Cassing, E.L. Bratkovskaya, Phys. Rep. 308 (1999) 65.
- [37] F. Laue, *et al.*, Phys. Rev. Lett. 82 (1999) 1640.
- [38] A. Förster, *et al.* (KaoS Collaboration), Phys. Rev. Lett. 91 (2003) 152301.
- [39] W. Scheinast, *et al.* Phys. Rev. Lett. 96 (2006) 072301.
- [40] J. Mareš, E. Friedman, A. Gal, Nucl. Phys. A 770 (2006) 84.
- [41] X.H. Zhong, G.X. Peng, L.Li, P.Z. Ning, Phys. Rev. C 74 (2006) 034321.
- [42] G.A. Lalazissis, J. König, P. Ring, Phys. Rev. C 55 (1997) 540.
- [43] B.G. Todd-Rutel, J. Piekarewicz, P.D. Cottle, Phys. Rev. C 69 (2004) 021301(R).

- [44] W.Z. Jiang, Y.L. Zhao, Z.Y. Zhu, S.F. Shen, Phys. Rev. C 72 (2005) 024313.
- [45] B.G. Todd-Rutel, J. Piekarewicz, Phys. Rev. Lett. 95 (2005) 122501.
- [46] F.J. Fattoyev, C.J. Horowitz, J. Piekarewicz, G. Shen, Phys. Rev. C 82 (2010) 055803.
- [47] P.G. Reinhard, M. Rufa, J. Maruhn, W. Greiner, J. Friedrich, Z. Phys. A 323 (1986) 13.
- [48] Y. Sugahara, H. Toki, Nucl. Phys. A 579 (1994) 557.
- [49] T. Nagae, JPS Conf. Proc. 17 (2017) 081001.
- [50] S. Ajimura, *et al.* (J-PARC E15 collaboration), Phys. Lett. B 789 (2019) 620.